Electronic Supplementary Material (ESI) for Dalton Transactions.

Electronic Supplementary Material

Fluorescent and Electrochemical Detection of Iodine Vapor in the Presence of High Humidity using Ln-based MOFs

Xiuting Dong,[a, b] Qing He,[a] Menglin Li,[a, b] Xinpeng Wang,[a, b] Yuxin Wang,[a, b] Wen Zhang*,[a, b]

[a]School of Chemical Engineering and Technology, Tianjin University, Tianjin 300350, China.

[b]State Key Laboratory of Chemical Engineering, Tianjin Key Laboratory of Membrane Science & Desalination Technology, Tianjin 300350, China.

*To whom correspondence should be addressed. zhang_wen@tju.edu.cn (W. Z.)

Table of Contents

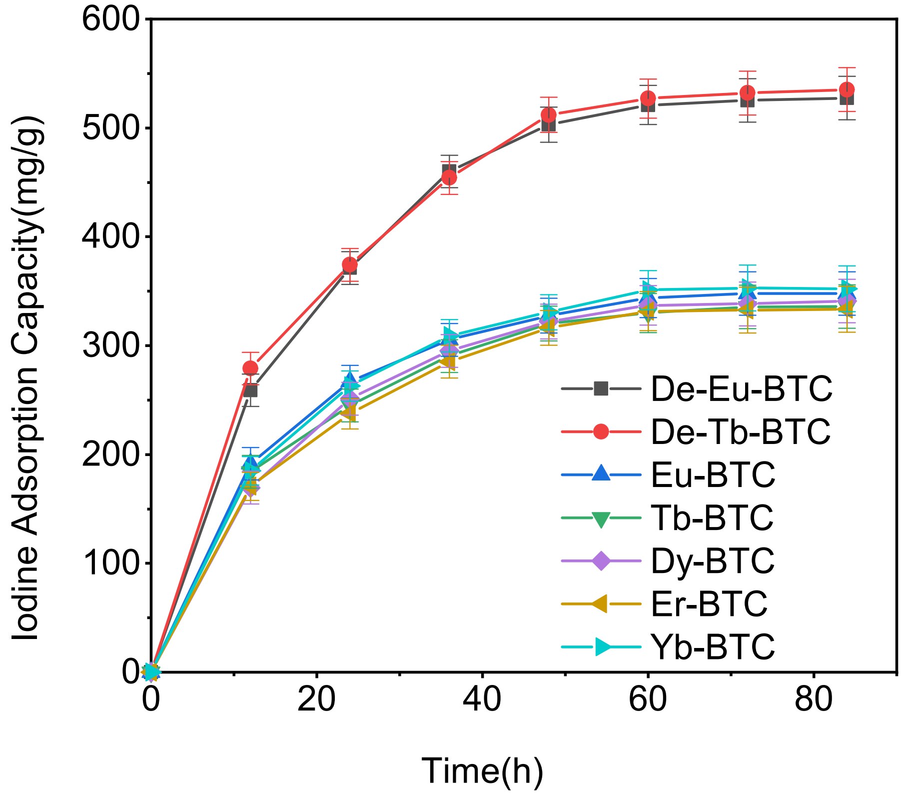

Figure S1. Adsorption curves of Ln-BTCs and De-Ln-BTCs in saturated iodine vapor at 80℃

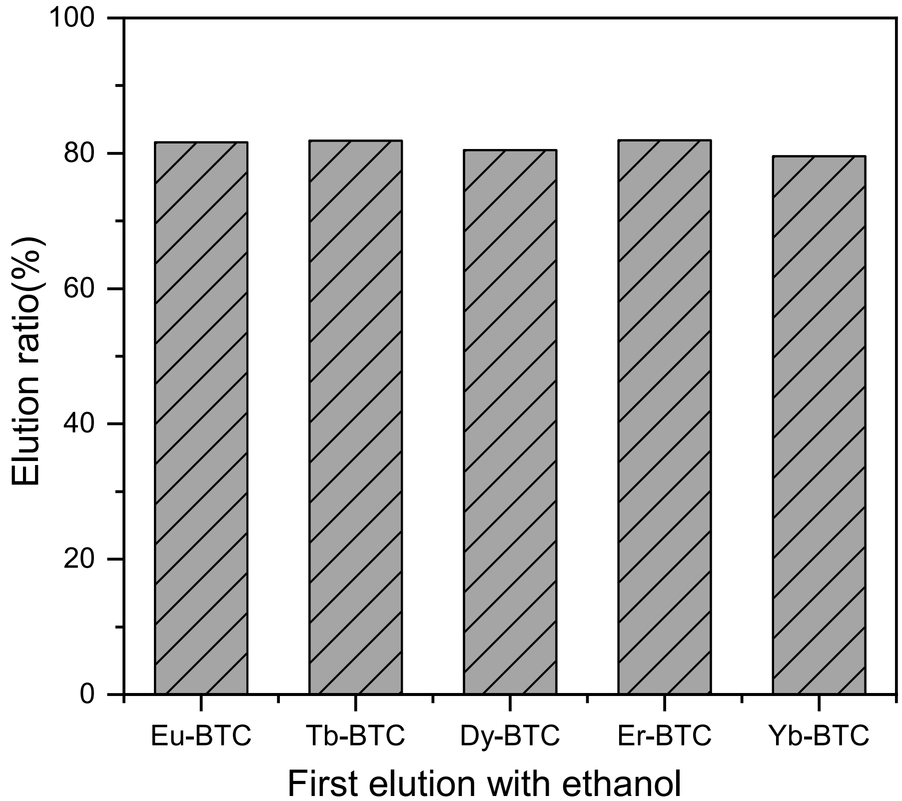

Figure S2. Elution ratios of adsorbed iodine via ethanol soaking

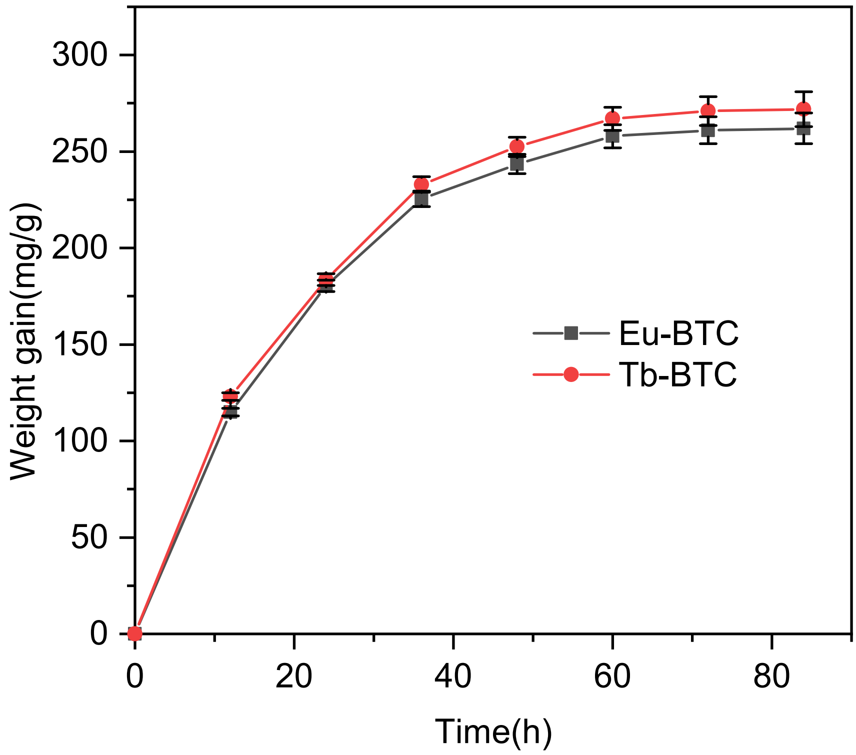

Figure S3. Adsorption curves of Ln-BTCs in saturated iodine vapor with 18% relative humidity at 80℃

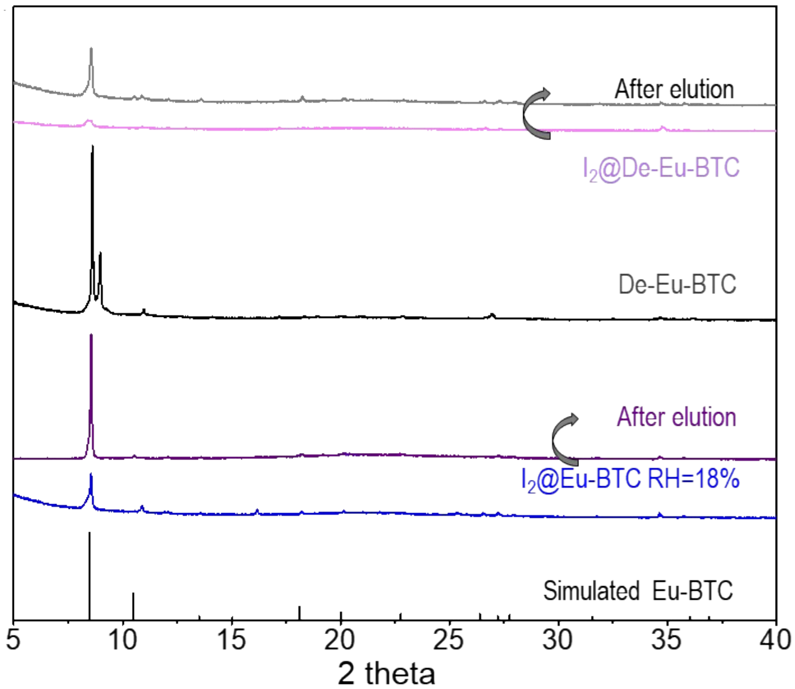

Figure S4. PXRD patterns of I_2@Eu-BTC under 18% relative humidity, De-Eu-BTC, I_2@De-Eu-BTC and iodine-loaded samples after elution.

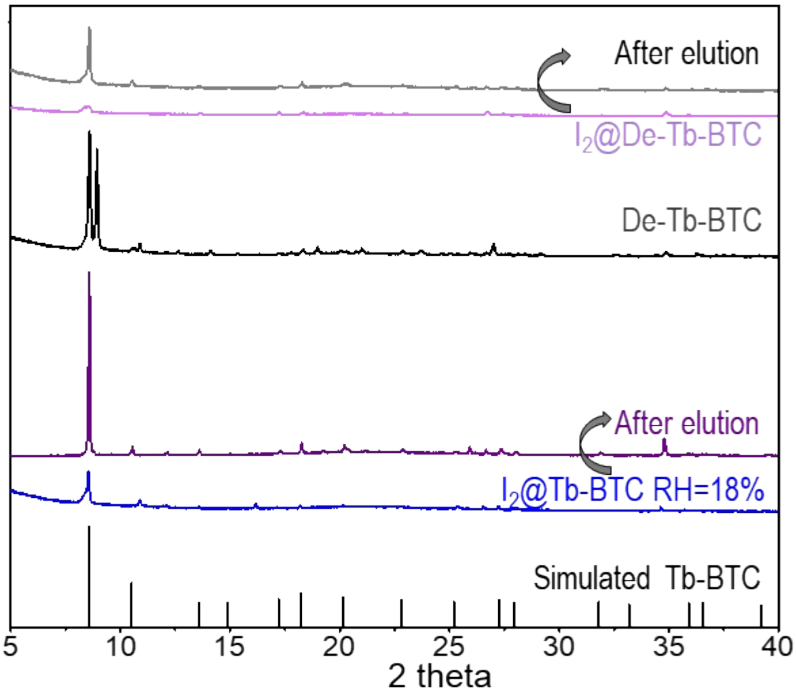

Figure S5. PXRD patterns of I_2@Tb-BTC under 18% relative humidity, De-Tb-BTC, I_2@De-Tb-BTC and iodine-loaded samples after elution.

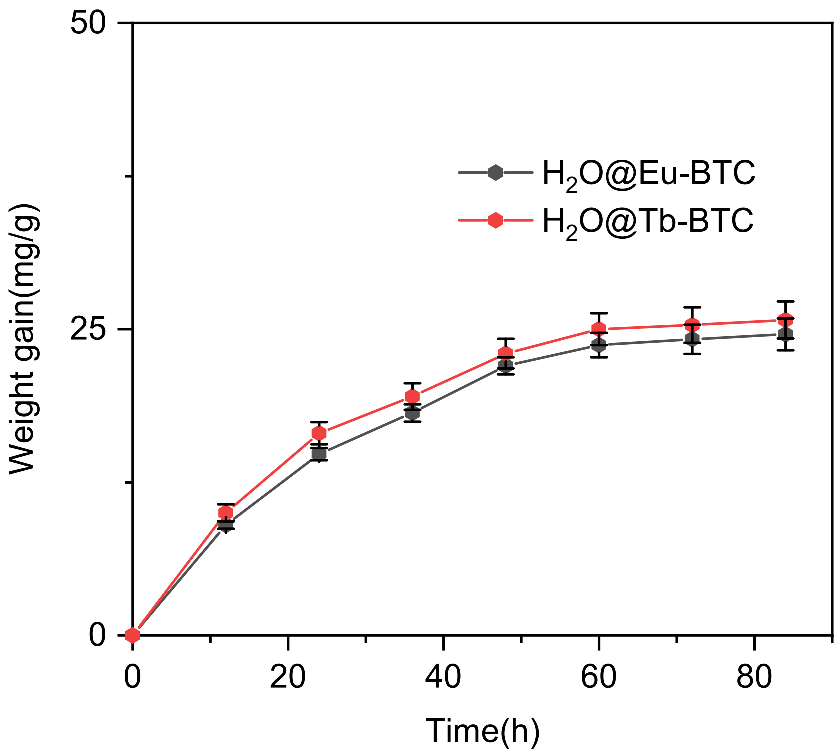

Figure S6. Water adsorption curves of Ln-BTCs in 18% relative humidity at 80 ℃
(The vial with 30 mg Ln-BTC was introduced into in a sealed bottle which contains 3 mL saturated calcium chloride aqueous solution. The bottle was placed in an 80 ℃ oven).

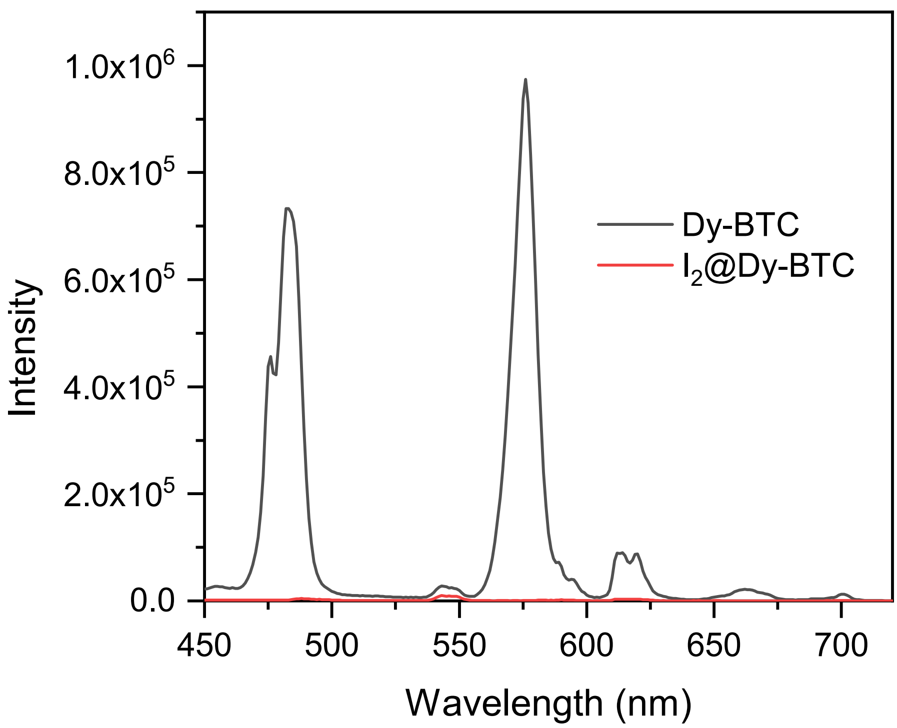

Figure S7. Emission spectra of I_2@Dy-BTC with an excitation wavelength of λ_{ex}=297 nm

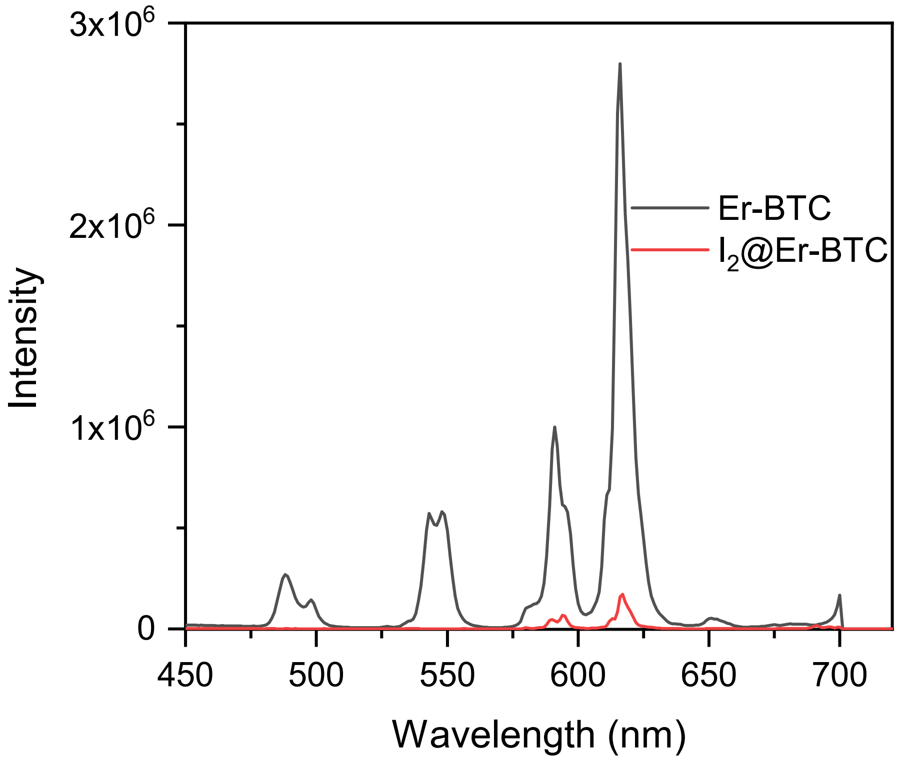

Figure S8. Emission spectra of I_2@Er-BTC with an excitation wavelength of λ_{ex}=297 nm

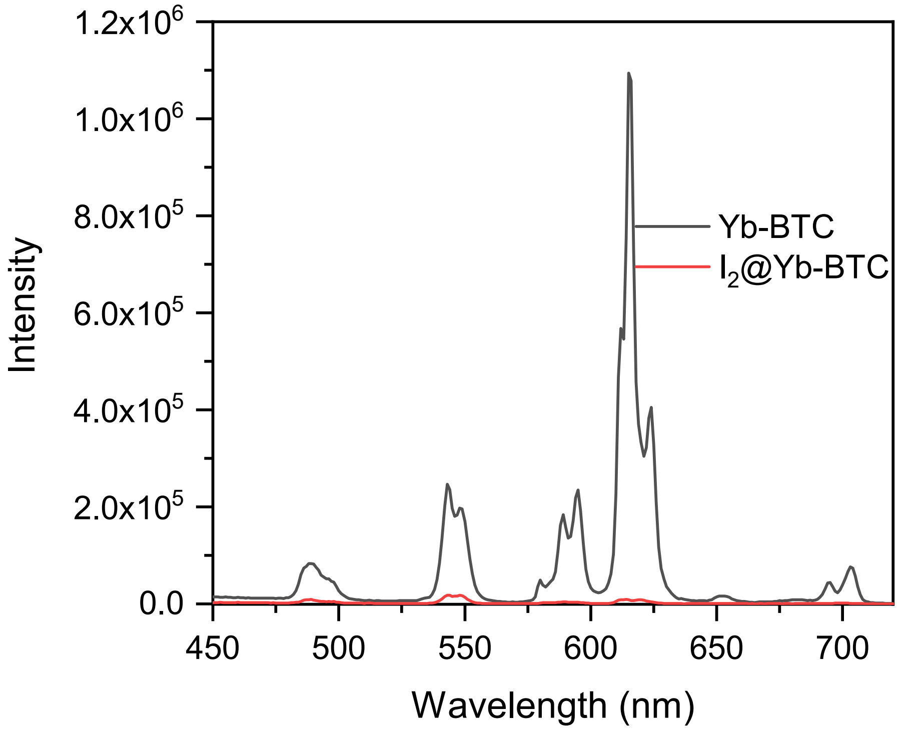

Figure S9. Emission spectra of I_2@Yb-BTC with an excitation wavelength of λ_{ex}=297 nm

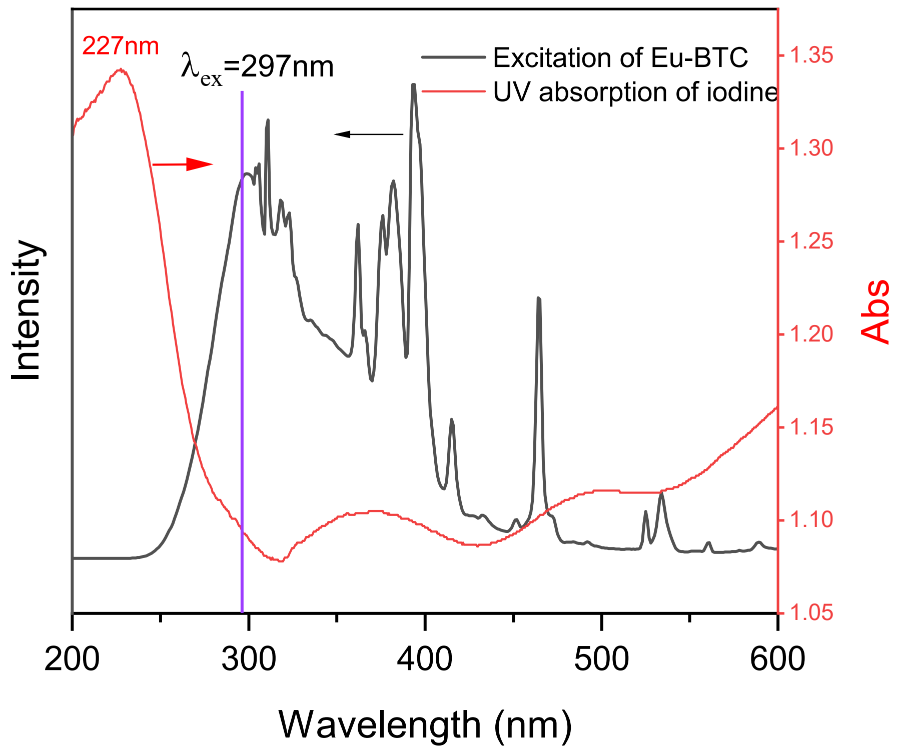

Figure S10. Solid-state UV-Vis spectrum of I_2 and emission spectrum of Eu-BTC

(The solid-state UV-Vis spectra of iodine was measured using a SHIMADZU UV-2600 UV-Vis-NIR spectrophotometer at room temperature. The excitation spectrum of Eu-BTC powder was measured using a Jobin Yvon Fluorolog3-21 coupled with a 400 nm longpass filter with a Xe 450W ozone-free continuous xenon arc lamp and a 2 nm slit width, monitored at 620 nm.)

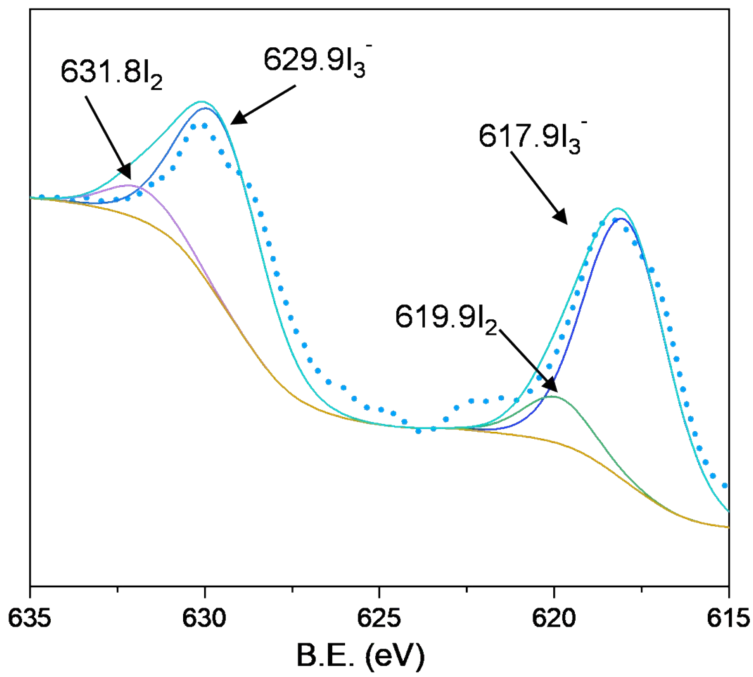

Figure S11. XPS spectra of I 3d in Iodine-loaded Eu-BTC after treating in vacuum for 12 h at 100 ℃ (X-ray photoelectron spectroscopy (XPS), Thermo ESCALAB 250Xi, C 1s at 285 eV)

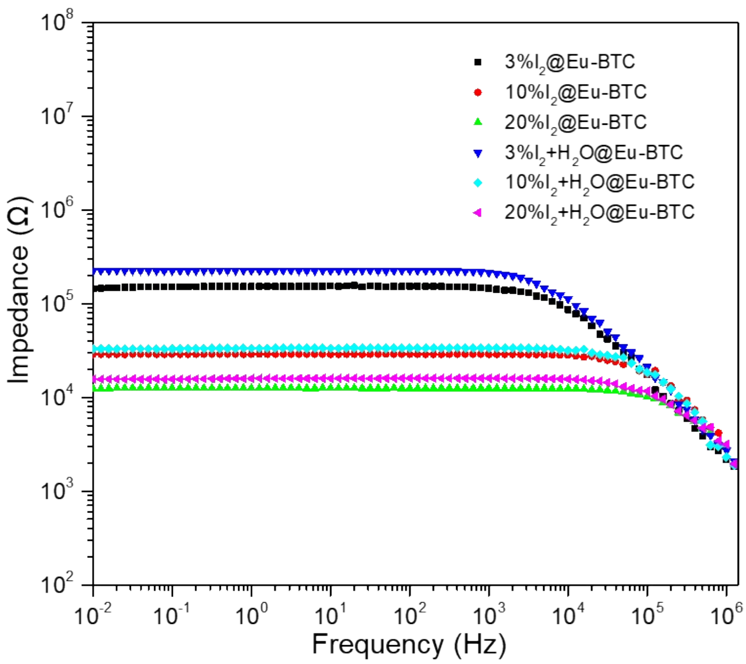

Figure S12. Impedance response plots of Eu-BTC upon iodine and/or water uptake with different weight percents

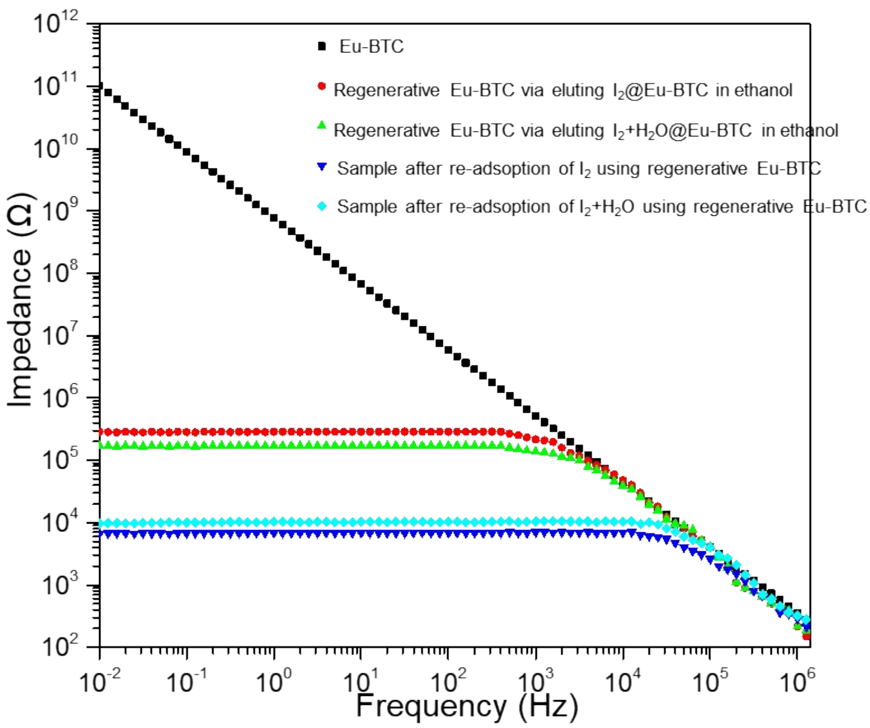

Figure S13. The reuse performance of Eu-BTC using impedance response

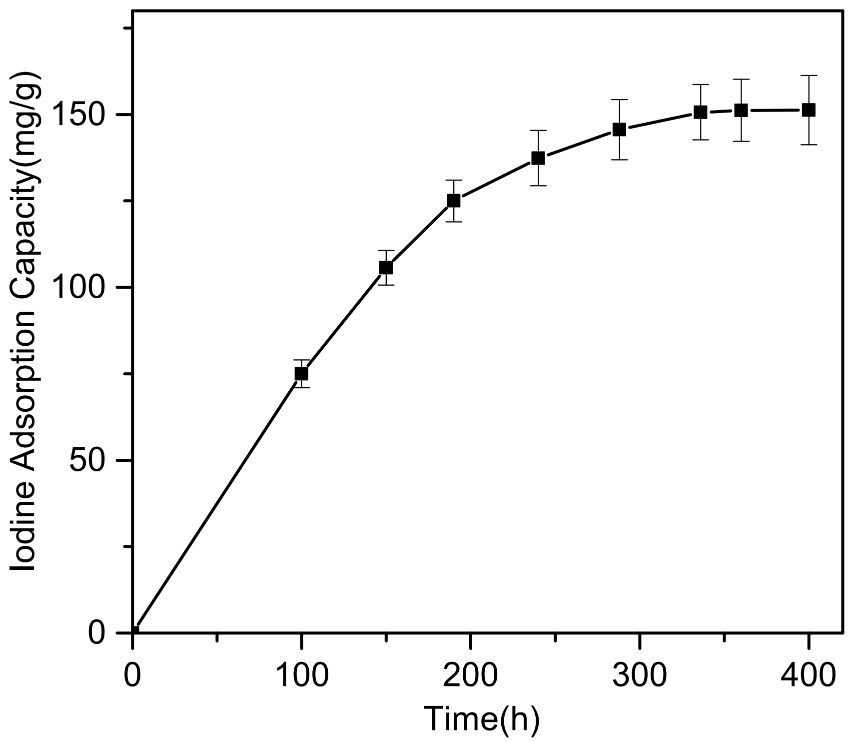

Figure S14. Adsorption curves of Eu-BTC monocrystal in saturated iodine vapor at 80 ℃
(A vial with 30 mg Ln-BTC monocrystal were introduced into in a sealed bottle which contains about 1.5 g solid iodine for iodine uptake. The bottle was placed in an oven and kept at 80 °C)

Table S1 Iodine-loading-induced increase of the electric conductivity for MOFs

MOFs	Iodine capability wt%	conductivity for MOFs (S/cm)	conductivity for I_2-loaded MOFs (S/cm)	Times	Ref
$Eu_4(BPT)_4(DMF)_2(H_2O)_8$	17.41	8.27×10^{-7}	2.71×10^{-5}	33	[1]
$\{(Na_2I_2CB[6])\cdot8H_2O\cdot1.4I_2\}$)	25	—	7.46×10^{-7}	—	[2]
$[Co_{1.5}(BDC)_{1.5}(H_2BPZ)]\cdot DMF\cdot4H_2O$	20.2	2.59×10^{-9}	7.69×10^{-6}	2.97×10^{3}	[3]
$[Tb(Cu_4I_4)(ina)_3(DMF)]$	22.6	5.72×10^{-11}	2.16×10^{-4}	3.78×10^{6}	[4]
ZIF-8	116	—	—	$\times10^{5}$	[5]
MFM-300(In)	15	—	—	$\times10^{6}$	[6]
MFM-300(V^{III})	—	1.7×10^{-10}	1.2×10^{-4}	7.06×10^{5}	[7]
$[Ca_2(TBAPy)(OH_2)_2]\cdot2DMF$	25	$<10^{-9}$	5.3×10^{-6}	$>10^{3}$	[8]
$[DMA][In(TDC)_2]$	56	1.3×10^{-11}	2.8×10^{-8}	2.15×10^{3}	[9]
dhMOF	17	2×10^{-8}	2.6×10^{-4}	1.30×10^{4}	[10]
Fe-MET-3	—	0.77×10^{-4}	1×10^{-3}	13	[11]
$Cu[Ni(pdt)_2$	—	1×10^{-8}	1.2×10^{-4}	1.20×10^{4}	[12]
$[Cu_6(pybz)_8(OH)_2]\cdot I_5^-\cdot I_7^-$	85	8.04×10^{-9}	8.11×10^{-7}	1×10^{2}	[13]
NiPc-CoTAA	—	8.16×10^{-3}	0.52	64	[14]
$[(Me_2NH_2)_2][Cd_3(5\text{-}tbip)_4]\cdot2DMF$	58	1.71×10^{-8}	1.29×10^{-6}	76	[15]
Eu-BTC (RH=0)	33.5	2.78×10^{-13}	6.08×10^{-6}	2.19×10^{7}	This work
Eu-BTC (RH=18%)	26.1	4.10×10^{-11}	1.55×10^{-6}	3.78×10^{4}	This work
Tb-BTC (RH=0)	34.8	3.78×10^{-13}	6.62×10^{-6}	1.75×10^{7}	This work
Tb-BTC (RH=18%)	27.2	4.57×10^{-11}	2.04×10^{-6}	4.51×10^{4}	This work

The calculation of electrical conductivity of Ln-BTC and I_2@Ln-BTC

The conductivity is calculated according to the following equations:

$$\sigma = \frac{L}{R\times A}$$

, where σ = conductivity (S/cm), R = resistance, A = cross sectional area of electrodes (cm^2), and L = distance between electrodes (cm).

References

[1] Hao, Z.; Yang, G.; Song, X.; Zhu, M.; Meng, X.; Zhao, S.; Song, S.; Zhang, H., A europium(III) based metal–organic framework: bifunctional properties related to sensing and electronic conductivity. *Journal of Materials Chemistry A* **2014**, 2 (1), 237-244.

[2] Lin, J.-X.; Liang, J.; Feng, J.-F.; Karadeniz, B.; Lü, J.; Cao, R., Iodine uptake and enhanced electrical conductivity in a porous coordination polymer based on cucurbit[6]uril. *Inorganic Chemistry Frontiers* **2016**, 3 (11), 1393-1397.

[3] Li, G. P.; Zhang, K.; Zhao, H. Y.; Hou, L.; Wang, Y. Y., Increased Electric Conductivity upon I2 Uptake and Gas Sorption in a Pillar-Layered Metal-Organic Framework. *Chempluschem* **2017**, 82 (5), 716-720.

[4] Hu, Y.-Q.; Li, M.-Q.; Wang, Y.; Zhang, T.; Liao, P.-Q.; Zheng, Z.; Chen, X.-M.; Zheng, Y.-Z., Direct Observation of Confined $I^{-}\cdots I_2\cdots I^{-}$ Interactions in a Metal–Organic Framework: Iodine Capture and Sensing. *Chemistry – A European Journal* **2017**, 23 (35), 8409-8413.

[5] Small, L. J.; Nenoff, T. M., Direct Electrical Detection of Iodine Gas by a Novel Metal-Organic-Framework-Based Sensor. *ACS Applied Materials & Interfaces* **2017**, 9 (51), 44649-44655.

[6] Small, L. J.; Hill, R. C.; Krumhansl, J. L.; Schindelholz, M. E.; Chen, Z.; Chapman, K. W.; Zhang, X.; Yang, S.; Schroder, M.; Nenoff, T. M., Reversible MOF-Based Sensors for the Electrical Detection of Iodine Gas. *ACS Applied Materials & Interfaces* **2019**, 11 (31), 27982-27988.

[7] Zhang, X.; da Silva, I.; Fazzi, R.; Sheveleva, A. M.; Han, X.; Spencer, B. F.; Sapchenko, S. A.; Tuna, F.; McInnes, E. J. L.; Li, M.; Yang, S.; Schroder, M., Iodine Adsorption in a Redox-Active Metal-Organic Framework: Electrical Conductivity Induced by Host-Guest Charge-Transfer. *Inorganic Chemistry* **2019**, 58 (20), 14145-14150.

[8] Gladysiak, A.; Nguyen, T. N.; Spodaryk, M.; Lee, J. H.; Neaton, J. B.; Zuttel, A.; Stylianou, K. C., Incarceration of Iodine in a Pyrene-Based Metal-Organic Framework. *Chemistry – A European Journal* **2019**, 25 (2), 501-506.

[9] Mani, P.; Mandal, N.; Roopesh, M.; Gopalakrishnan, H.; Datta, A.; Mandal, S., Enhancement in electrical conductivity of a porous indium based metal–organic framework upon I_2 uptake: combined experimental and theoretical investigations. *Journal of Materials Chemistry C* **2020**, 8 (14), 4836-4842.

[10] Gordillo, M. A.; Benavides, P. A.; Panda, D. K.; Saha, S., The Advent of Electrically Conducting Double-Helical Metal-Organic Frameworks Featuring Butterfly-Shaped Electron-Rich pi-Extended Tetrathiafulvalene Ligands. *ACS Applied Materials & Interfaces* **2020**, 12 (11), 12955-12961.

[11] Gandara, F.; Uribe-Romo, F. J.; Britt, D. K.; Furukawa, H.; Lei, L.; Cheng, R.; Duan, X.; O'Keeffe, M.; Yaghi, O. M., Porous, conductive metal-triazolates and their structural elucidation by the charge-flipping method. *Chemistry – A European Journal* **2012**, 18 (34), 10595-601.

[12] Kobayashi, Y.; Jacobs, B.; Allendorf, M. D.; Long, J. R., Conductivity, Doping, and Redox Chemistry of a Microporous Dithiolene-Based Metal−Organic Framework. *Chemistry of Materials* **2010**, 22 (14), 4120-4122.

[13] Yin, Z.; Wang, Q. X.; Zeng, M. H., Iodine release and recovery, influence of polyiodide anions on electrical conductivity and nonlinear optical activity in an interdigitated and interpenetrated bipillared-bilayer metal-organic framework. *Journal of the American Chemical Society* **2012**, 134 (10), 4857-63.

[14] Yue, Y.; Cai, P.; Xu, X.; Li, H.; Chen, H.; Zhou, H. C.; Huang, N., Conductive Metallophthalocyanine Framework Films with High Carrier Mobility as Efficient Chemiresistors. *Angewandte Chemie International Edition* **2021**, 60 (19), 10806-10813.

[15] Chaudhari, A. K.; Mukherjee, S.; Nagarkar, S. S.; Joarder, B.; Ghosh, S. K., Bi-porous metal–organic framework with hydrophilic and hydrophobic channels: selective gas sorption and reversible iodine uptake studies. *CrystEngComm* **2013**, 15 (45), 9465.